

## Putative Binding Sites of Dopamine and Arachidonoyl Dopamine to Beta-lactoglobulin: A Molecular Docking and Molecular Dynamics Study

S. Gholami and A.K. Bordbar\*

*Department of Chemistry, University of Isfahan, Isfahan 81746-73441, Iran*

*(Received 15 July 2016, Accepted 7 November 2016)*

Because of participation in many aspects of human life, and due to oxidation-sensitive characteristics of dopamine (DA) and arachidonoyl dopamine (AA-DA), the necessity of biocompatible carrier to keep them against oxidation is of importance. In this work, we explored the putative binding sites of DA and AA-DA to  $\beta$ -lactoglobulin (BLG) as potent carrier. Docking results identified the binding sites, involved residues and driving forces to the binding process of these ligands. The dissimilar binding site of AA-DA in comparison with DA has been designated by different values of Gibbs free energy, binding constants and contact residues. Molecular dynamics simulation outcomes confirmed that both compounds stayed in their predicted binding sites during the entire time of simulation with no major secondary and tertiary protein structural changes indicating that BLG might be considered as a suitable oxidation-protective carrier for these compounds.

**Keywords:** Dopamine, Arachidonoyl dopamine, Binding site, Molecular docking, Molecular dynamics simulation

### INTRODUCTION

Dopamine (DA), a catecholamine neurotransmitter found in neurons of both the central and peripheral nervous systems, is one of the most studied biogenic amines in animal organism. DA signaling properties comprise various activities, linked to attention, set-shifting, working memory, reward, as well as to other cognitive functions and mood [1]. Dopamine, also, has important roles in cardiovascular regulation through its effects on blood vessels and its renal actions [2]. Several important nervous system diseases are related to the dopamine system dysfunction, consequently, some of the main drugs used to treat them are associated with the adjustment of its effects. Parkinson's disease is caused by a loss of dopamine-secreting neurons, as this catecholamine plays a critical role in the regulation of our movements and is thought to be a crucial part of the basal ganglia motor loop. Its metabolic precursor L-DOPA can be produced, and in its pure form marketed as Levodopa is the

most widely used treatment for the condition. In schizophrenia, there are signs that demonstrate the level of dopamine activity changes. Most of the drugs used to treat schizophrenia disease are dopamine antagonists which reduce dopamine activity [3].

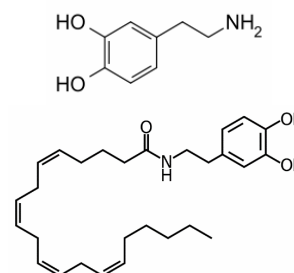
Arachidonoyl dopamine, AA-DA, as a lipophilic analogue of dopamine with promising applications in biochemistry and drug design, along with other natural N-acyl dopamines carrying oleic, docosahexaenoic, palmitic and stearic acids are thought to function within cannabinoid-vanilloid system, primarily affecting neuronal plasticity, pain transduction and immune response (for review see [1]). The targets of N-acyl dopamines are vanilloid receptor TRPV1 (activation), cannabinoid receptor CB1 (activation), calcium channels CaV3 (inhibition), potassium channels TASK3 (inhibition) as well as several intracellular proteins [1]. In some cell-based test systems, N-acyl dopamines produce comparable effects in comparison with N-arachidonoyl noradrenaline, [4] that along with endogenous N-arachidonoyl serotonin, N-arachidonoyl glycine and N-arachidonoyl gamma

\*Corresponding author. E-mail: [bordbar@chem.ui.ac.ir](mailto:bordbar@chem.ui.ac.ir)

aminobutyric acid form a family of acyl neurotransmitters closely related to endocannabinoids.

It has been proved by experimental evidence that oxidizing the catecholamines to aminochromes as a result of their excessive amounts of circulation, can lead to some disorders such as intracellular  $\text{Ca}^{2+}$ -overload, coronary spasm, myocardial cell damage, depletion of high energy stores, and ventricular arrhythmias. In addition, the formation of oxyradicals during the oxidation process may play a critical role in the genesis of ventricular arrhythmias that may result in sudden cardiac death [5]. The reactive quinones are formed from acylated catecholamines too [6]. Consequently, they must be sheltered from oxidant agents which could affect their physiological advantages. The binding of these compounds to carrier proteins can protect them from oxidation. Bovine  $\beta$ -lactoglobulin (BLG), an abundant milk protein, makes up to 50% of whey and 12% of whole cow milk proteins [7] belongs to the lipocalin proteins which can bind with many ligands and drugs such as fatty acids, lipids, aromatic compounds, vitamins and polyamines [8-10]. Alternatively, protection of some ligands from oxidation, due to their binding with BLG, suggests that this protein could be employed as an effective carrier of oxidation-sensitive drugs [11]. It has been discovered that binding of folic acid to BLG improves its photostability [8]. Also, it has been shown that epigallocatechin-3-gallate (EGCG) in thermally-induced BLG-EGCG conjugates are protected from oxidative degradation [12]. Because of good biocompatibility and biodegradability of milk proteins, BLG could be considered as natural carrier for lipid-soluble drugs [13,14] and hence would be a candidate for carrying of DA and AA-DA and related compounds in controlled drug delivery.

Due to the biological and pharmaceutical importance of DA and AA-DA, here, we reported the structural and dynamic changes of BLG-DA and BLG-(AA-DA) with the intention of evaluating the possible ability of BLG for carrying of these precious ligand by using molecular docking and molecular dynamic simulation techniques. Concerning to the absence of any comprehensive computational study on these systems in the literature, the results of this study would be useful in designing the effective and protective carrier for these biological important compounds.



*Scheme 1.* Chemical structures of DA (top) and AA-DA (bottom)

## COMPUTATIONAL DETAILS

### Molecular Docking

Molecular docking was performed with unliganded form of BLG (variant B; PDB ID: 3NPO) (<http://www.rcsb.org/pdb>) as receptor structure using AutoDock 4.2 program package. Water molecules were removed from the structure of protein and Gasteiger charges and missing hydrogen atoms were added to the BLG in AutoDock Tools environment. The structure of ligands was minimized by the quantum chemistry package Gaussian 03 using Hartree-Fock method and 6-31G(d,p) basis set to get the optimized and stable geometry [15]. The structure with the lowest energy was chosen as initial geometry for docking study.

As there is no any prior knowledge of DA and AA-DA binding site, firstly, protein-ligand docking was performed on the whole protein surface as a potential binding site with grid size of  $126 \times 126 \times 126$  along  $X, Y, Z$  axes and a grid point spacing of  $0.375 \text{ \AA}$ . The ligand binding sites were predicted based on the docking scores of the ligands. Subsequently, binding location was defined by a docking box of  $60 \times 60 \times 60$  dimensions and a grid point spacing of  $0.375 \text{ \AA}$ . All docking computations were performed using the AutoDock empirical free energy function and the Lamarckian genetic algorithm with local search [16]. Electrostatic and van der Waals interactions, hydrogen bonding and entropy losses were considered for energy based Autodock scoring function. For each docking calculation, a pool of 200 independent conformations were generated and assessed with 25,000,000 energy evaluations while the default values were used for all other docking parameters. The resulting docked structures were clustered with a RMSD tolerance criterion of  $2.0 \text{ \AA}$ . The complex

configuration with the best docking score was selected for further analysis amongst the several binding mode generated based on docking scores.

### **Molecular Dynamics Simulation**

Although, docking analysis provides the information about the binding modes of ligands, the binding energy and the residues of protein in close contact to the ligand binding location, the accurate characterization of the structure and dynamics of protein in bound state cannot be explained by such static docking simulation. Molecular dynamics (MD) simulations allow us to inquire the structure and dynamics of protein in both free and bound states with the intention of confirming the main binding mode confirmation and getting the impression of the ligand in the binding site of BLG, such as the probable conformational changes and the stability of complex during the binding. To this end, the obtained geometry with the lowest energy from docking was used as starting conformation for MD study.

All three systems (free BLG, BLG-DA and BLG-(AA-DA)) were solvated in a box of 294 nm<sup>3</sup> containing 8895 single point charge (SPC) [17] water molecules. Seven Na<sup>+</sup> as the appropriate number of counter-ions, were added to the simulation box to make the systems electrically neutral and subsequently, 3D periodic boundary conditions were applied. We used the GROMACS 4.5.4 package [18] with the GROMOS96 43a1 force field [19] for protein, waters and ions, and PRODRG web server [20] to export the ligands topology parameters. A 1.0 nm cutoff was used for the Lennard-Jones and short-range electrostatic interactions; long-range electrostatic interactions were treated with the Particle Mesh Ewald (PME) method [21,22] using 1.0 nm cut off.

Following standard procedures for system equilibration, the energy of the systems was first minimized by using the steepest descent method to facilitate the systems to be relaxed and to relieve unfavorable conflicting contacts. MD simulation studies comprised of equilibration and production phases. In the equilibration phase a 100 ps MD simulation in the NVT ensemble was carried to equilibrate the systems at 300 K with the Nose-Hoover thermostat coupling method [23,24] which was followed by a 100 ps NPT equilibration using the Parrinello-Rahman barostat [25] to keep pressure constant in 1.0 bar. After

equilibration, trajectories with a length of 15 ns were recorded using the leap-frog algorithm for solving the equations of motion [26] with a time step of 2 fs. The trajectory files were analyzed by using `g_rmsd`, `g_rmsf`, `g_gyrate`, and `g_sas` GROMACS utilities to obtain the root mean square displacement, RMSD, root mean square fluctuations, RMSF, radius of gyration, Rg and solvent accessible surface area, SASA. The number of distinct intermolecular hydrogen bonds formed during the simulation was calculated using `g_hbond` utility. Using DSSP module secondary structural analyses were performed for both free and bound BLG. Moreover, principal component analysis was applied to determine the most important motions contributing to the overall dynamics of the protein with the use of `g_covar` and `g_anaeig` of GROMACS utilities. All the plots were prepared by SIGMAPLOT and XMGRACE tools.

## **RESULTS AND DISCUSSION**

### **Protein-ligand Interaction Results**

Three potential binding sites have been recognized for ligand binding to BLG. Among them, the internal cavity of the  $\beta$ -barrel (calyx), common to all lipocalins, has been known as the main binding site of BLG. Hydrophobic molecules such as fatty acids, vitamins, particularly vitamin D, retinol and palmitate have been proved to bind in calyx [27-29]. However, there are at least two distinct binding modes [9,30] for ligands in between the alpha-helix and beta-barrel; the surface hydrophobic pocket in a groove between the  $\alpha$ -helix and the  $\beta$ -barrel [31,32] and the third known binding site of BLG is located in the outer surface near Trp19-Arg124 [33,34]. Polar aromatic compounds, such as *p*-nitrophenyl phosphate, 5-fluorocytosine, ellipticine, and protoporphyrin, bind to outer surface site [31-34].

DA and AA-DA were docked to the BLG to determine the preferred binding sites on the protein and to understand the binding process in atomistic details as well as to identify key interactions involved in the complex formation. To predict possible binding modes, a blind molecular docking computation was performed. The docked conformations were ranked in order of increasing energy, called clustering. Cluster analysis predicted 18 and 109 different clusters for

**Table 1.** Involved Amino Acid Residues, Free Binding Energy, Relevant Binding Constant and Number of H-Bonds in BLG-DA and BLG-(AA-DaA) Interaction

Molecule	Residues identified to interact with ligand	$\Delta G^\circ$ , (kJ mol <sup>-1</sup> )	$K_a$ (10 <sup>5</sup> M <sup>-1</sup> )	No. of H-bonds
DA	Thr (18), Trp (19), Tyr (20), Ser (21), Glu (44), Gln (59), Leu (156), Glu (157), Glu (158), His (161)	-31.97	4.00	4
AA-DA	Val (41), Leu (54), Ile (71), Asn (90), Val (92), Phe (105), Met (107), Glu (108), Ser (116), Leu (117)	-39.50	83.57	1

binding modes of DA and AA-DA to the BLG, respectively. The large number of clusters in AA-DA case could be as a result of the high flexibility of this long polyene hydrophobic chain arachidonic derivative in its structure, which results in possibility of multiple biologically relevant conformations, particularly those in a bent form.

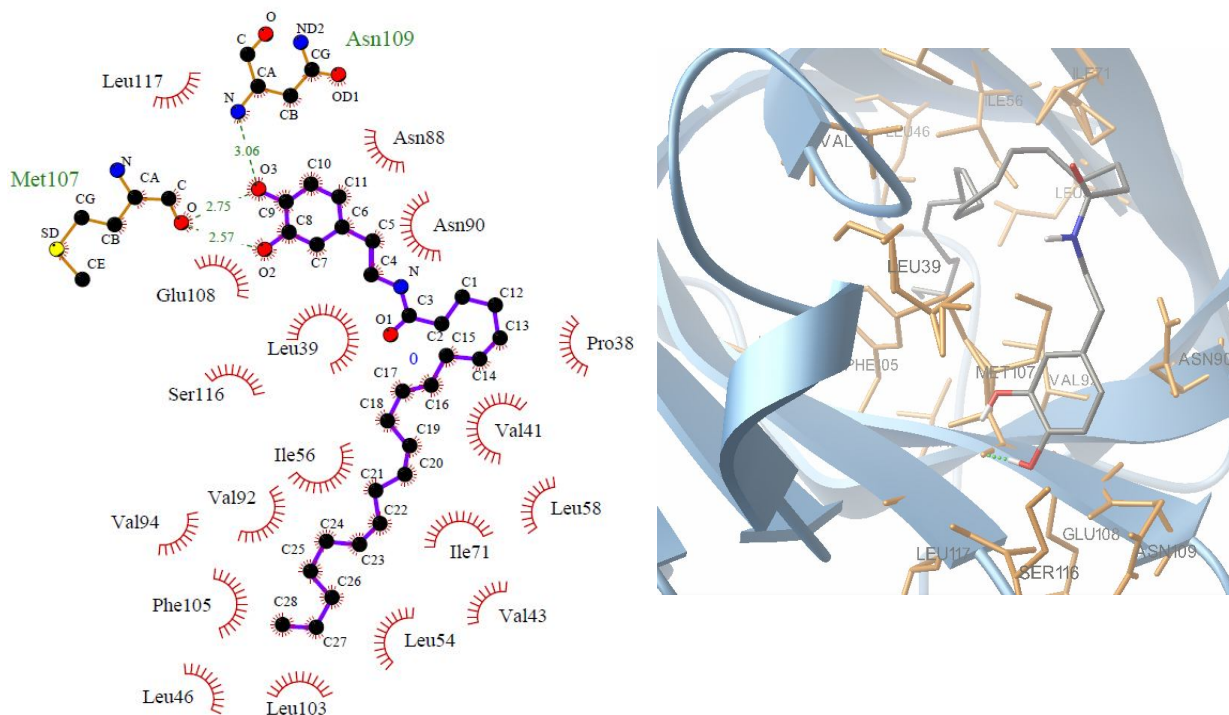
Our docking results showed that AA-DA docked in the calyx in all of the top-ranked docking poses (20 poses), with binding energies from -39.50 to -29.96 kJ mol<sup>-1</sup>. At this pose, AA-DA is surrounded by hydrophobic residues such as Leu, Phe, Val, Ile, Pro, and polar residues such as Asn, Ser, Met (2.75 Å = H-bond). Identified interacting residues, free binding energy, binding constant, and number of H-bonds for docked pose belonging to the first top-ranked cluster are listed in Table 1, and shown in Fig. 1 for AA-DA. Taking into account the involved residues to the binding of AA-DA to the BLG besides the H-bond interactions, the hydrophobicity of the fatty acid chain of AA-DA may be considered as the central driving force behind binding to BLG. The experimental evidence corresponding to open conformation of the internal hydrophobic calyx at pH 7.4 [35] is in agreement with this result.

Our docking results showed that DA does not dock preferentially at the calyx, instead being found at the outer surface site (third site) in the 9/18 of the top-ranked poses with binding energies from -31.97 to -27.40 kJ mol<sup>-1</sup> (Table 1, Fig. 2). The docking results demonstrate that DA is located near polar residues such as Tyr, Thr, Trp, Gln, His


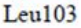


and negatively charged residue Glu. These results are in good agreement with experimental evidences suggesting the predominant role of both charge effects and hydrophobicity in determination of binding location of small molecules in the proteins [30]. At physiological pH, BLG is in the above of its isoelectric point (pH 5.26) and has negative charge, consequently, the positively charged ligands such as DA would be qualified to bind to the negatively charged site on the surface of BLG at this pH. It looks charge effects favor binding of DA to BLG.

The precise inspection of the binding mode of DA in the predicted binding site represents the formation of four hydrogen bonds. Actually, the polar atoms of DA (N and O) are in close contact with the protein and were anchored in the binding site by four H-bonds with the Glu (44) (3.17 Å = H-bond), Gln (59) (2.99 Å = H-bond and 3.01 Å = H-bond), and His (161) (2.66 Å = H-bond) (Fig. 2). Hence, it can be concluded that both electrostatic interactions and H-bonds are the main driving forces in the formation of DA-BLG complex. The attachment of DA and AA-DA to dissimilar binding sites led to different driving binding forces.

In the following, an unrestrained MD simulations is applied to provide a means for studying the dynamics and interactions of protein with ligand in the presence of explicit solvent. To do so, binding poses with the lowest docked energy belonging to the top-ranked cluster (pose 1) were selected for a more accurate docking with 60 × 60 × 60 grid and the resulting coordinates were used to molecular



Key:

-  Non ligand residues involved in the hydrophobic contacts
-  Leu103
-  Ligand bond
-  Non-ligand bond

**Fig. 1.** (Right) Three-dimensional view of the possible interacting model and binding site created by VMD, (Left) Two-dimensional schematic representation of hydrogen bonds and the main residues involved in the interaction of AA-DA with BLG. Dashed green lines represent the predicted H-bonds.

dynamics simulation refinements.

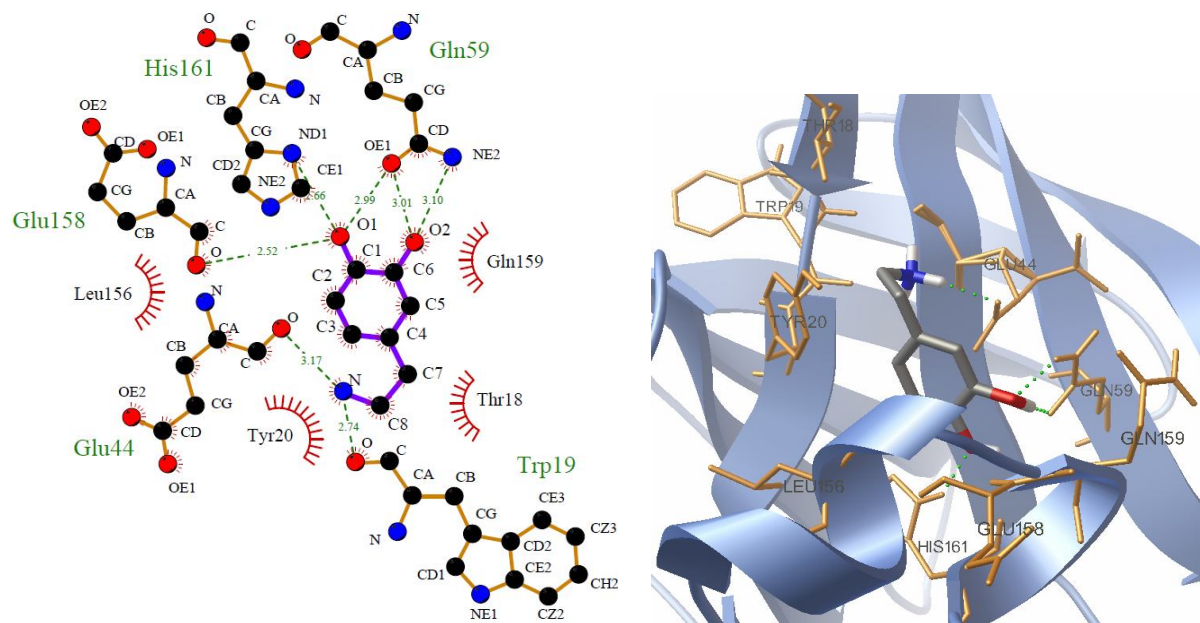
### Molecular Dynamics Simulation

The lowest energy structures resulting from docking were selected as the final model for post-docking analysis (15 ns MD simulation) of DA and AA-DA to BLG. To compare the structural stability of free and bound ligand BLG, and determination of the types of interaction involving in the binding reaction, some dynamic structural

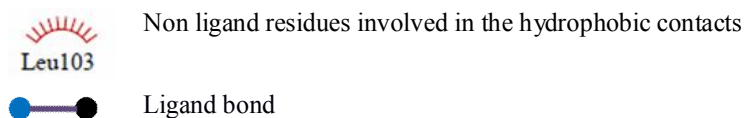
properties such as RMSD, RMSF, Rg, SASA, H-Bonds interactions, secondary structure and PCA were analyzed, that the detailed calculating results of these parameters are presented in the following subsections.

**Flexibility of protein and ligand molecules.** The trajectory stability of all systems could be checked by the analysis of the C $\alpha$  RMSD of protein from the initial structure, as a function of time. Concerning to the Fig. 3A, it can be concluded that the trajectories of free and bound





Key:

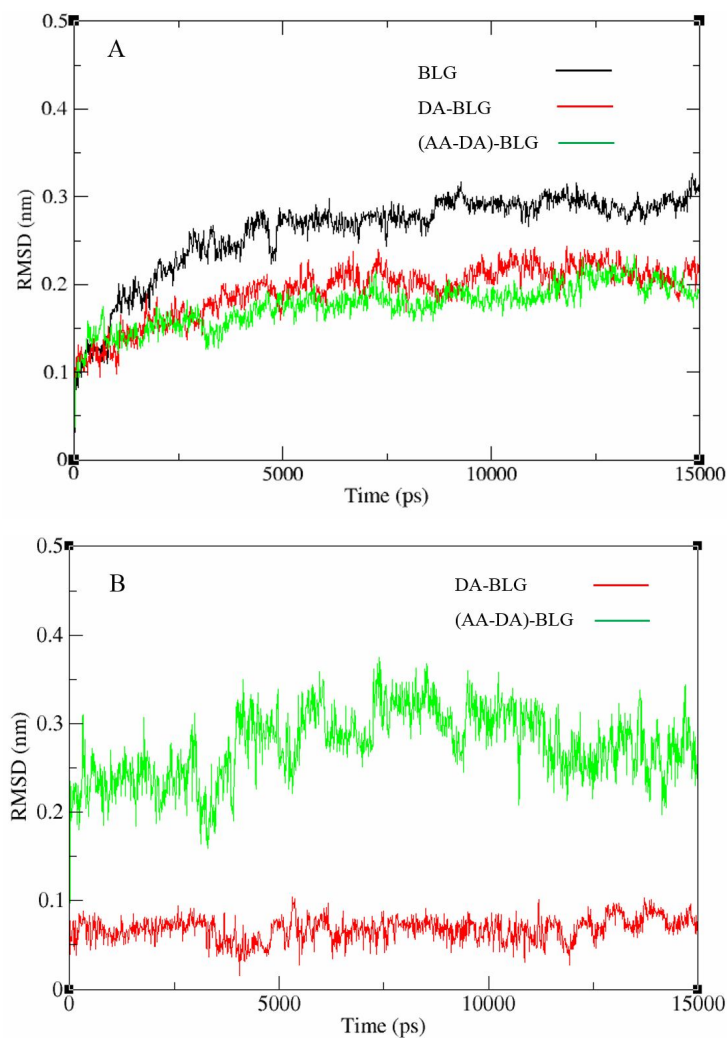


**Fig. 2.** (Right) Three-dimensional view of the possible interacting model and binding site, created by VMD (Left) Two-dimensional schematic representation of hydrogen bonds, and the main residues involved in the interaction of DA with BLG. Dashed green lines represent the predicted H-bonds.

BLG are stable after 5000 ps. In this plot, it is clear that there are slight structural re-organization in the first 5000-ps simulation time and then, short range oscillation in the RMSD around the average value after this time is traceable. In the other word, the RMSD of protein backbone atoms shows the similar trends for all three systems indicating the stability and equilibration during 5000 to 15000 ps simulation time. The mean RMSD values of protein backbone atoms from last 10000 ps trajectory were  $0.2854 \pm 0.0128$ ,  $0.1180 \pm 0.0160$ , and  $0.1760 \pm 0.0240$  nm for free BLG, BLG-DA and BLG-(AA-DA), respectively. The lower mean RMSD value of complexes shows that binding

of both ligands to the BLG decreases the degrees of freedom for protein motions. The magnitude of the fluctuations around the mean value, accompanied by small difference in the average RMSD values could be signified the stability of simulation trajectory, and consequently providing a suitable basis for further investigations.

In order to inspect the conformational variations of the ligands within the binding site, the RMSD of the atomic positions of ligands with respect to the starting structure was also calculated and shown in Fig. 3B. Concerning to this figure, the RMSD of DA leveled off during all the time of simulation and oscillated around the small mean value of

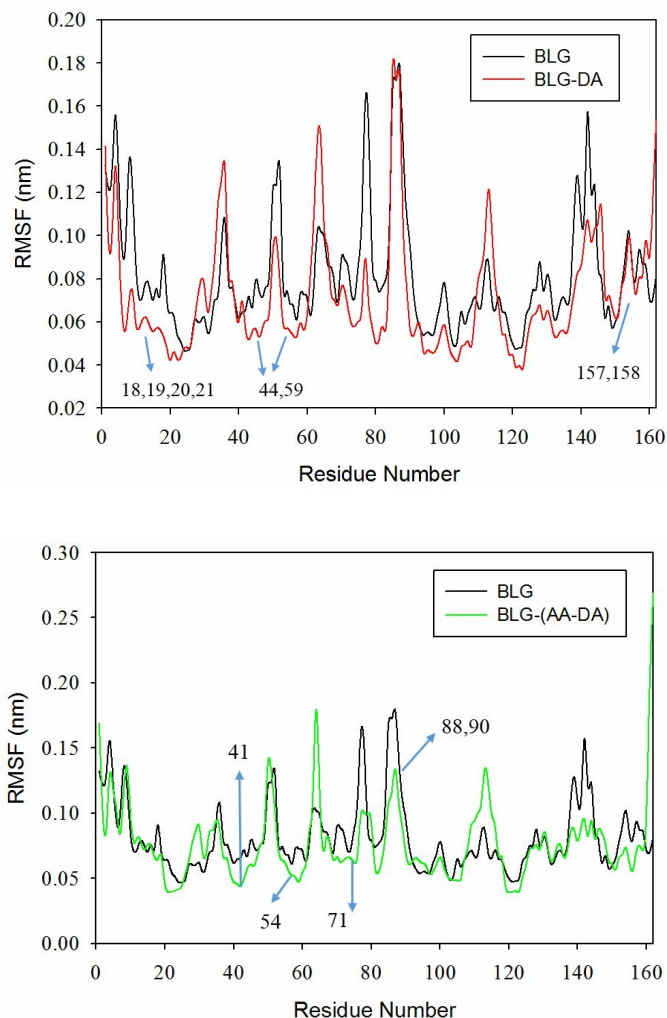


**Fig. 3.** (A) C $\alpha$  RMSD plots of BLG in free and bound states with DA and AA-DA. The lower RMSD value in the presence of ligands represents the formation of stable complexes. (B) RMSD of all atoms in ligands in the binding site of BLG with respect to their starting structure.

0.066 nm. This indicates an insignificant fluctuation in atoms of ligand, probably due to the large number of hydrogen bonds between the DA and BLG and the strong electrostatic interactions according to the +1 charge of the DA molecule. In contrast to DA, it can be seen that the RMSD of AA-DA undergoes larger movements. The RMSD value of AA-DA converged and equilibrated after 5000 ps, and then fluctuated around the mean value of  $0.230 \pm 0.033$  nm that is significantly higher than the corresponding value for DA. It could be due to the high-

flexible characteristics of this arachidonic-based compound during the MD trajectory.

**Root mean square fluctuations.** To measure the effect of complexation on the structural flexibility, dynamics and local mobility of protein, the time-averaged RMSF values for C $\alpha$  residues of free and bound BLG were computed. The results were plotted versus residue numbers and shown in Fig. 4. The presence of higher degrees of flexibility and fluctuation in free BLG compared to the bound protein represents the restriction of the conformational space of



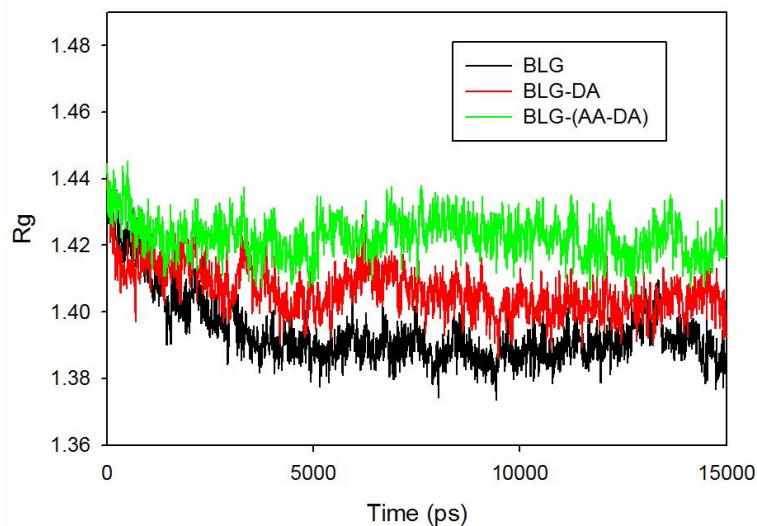
**Fig. 4.** RMSF of BLG residues with respect to their time-averaged positions for free and bound BLG. RMSF reductions in regions that directly in contact with ligands are shown with arrows.

BLG due to the binding process. In the other word, overall reduction in the RMSF values, in the case of BLG complexes, suggests that ligand binding induced constrains in the flexibility of protein structure and makes the backbone more rigid. The particular regions that are directly in contact with ligand (pointed in Fig. 4) showed more significant reduction of the RMSF due to intermolecular interactions of these residues with the ligands in the simulation time.

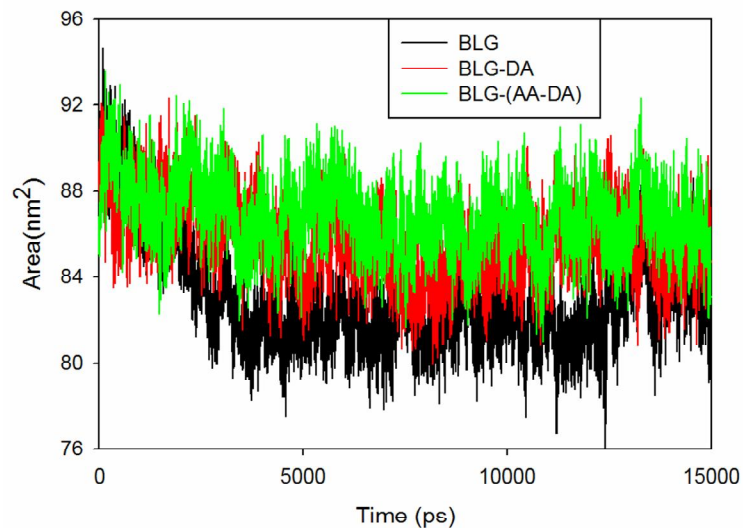
**Radius of gyration.** To have a quantitatively measure of the compactness, shape and folding of a protein structure,

the time evolution of the radius of gyration ( $R_g$ ) can be monitored due to its consideration as the mass-weighted root mean square distance of atoms from their center of mass. Actually, this quality could be regarded as a good assessment of the protein collapse dynamics. The  $R_g$  values for the free and bound form of protein were determined and plotted as a function of time, as shown in Fig. 5. The  $R_g$  patterns of free and bound BLG show a bit difference, with the  $R_g$  values decaying markedly during the simulation for the unbound protein and less so for the DA-bound protein. BLG-(AA-DA) complex showed a higher deviation with





**Fig. 5.** Gyration radius profiles of free and bound BLG. The increasing of  $R_g$  for complex represents the reducing of protein compactness due to complexation.



**Fig. 6.** Computed solvent accessible surface of free and bound BLG during 15 ns simulation time.

respect to the free BLG implying the more dynamic collapse of calyx in comparison with the surface binding site of DA. All systems were stabilized in  $R_g$  values at about 5000 ps, indicating that the MD simulation achieved equilibrium after this time. The higher mean value of  $R_g$  for complexes represented the reducing of protein compactness due to

complexation.

**Solvent accessible surface area.** The solvent-accessible surface area (SASA) is the surface area of a biomolecule that is accessible to a solvent which was firstly described by Lee & Richards in 1971 and is sometimes called the Lee-Richards molecular surface [36]. To quantify the effect of

binding process on compactness of the hydrophobic cores of protein, the change in SASA quantity could be measured. The SASA variations of the free and bound BLG with DA and AA-DA versus time are shown in Fig. 6. The created plots indicate higher values of SASA for bound BLG (85.20 and 86.50 nm<sup>2</sup> in the case of DA and AA-DA binding, respectively) when compared to free BLG (82.30 nm<sup>2</sup>) which supplies the impact of the binding on the protein structure in terms of increasing the solvent exposure. A main contributor to the increased exposure may be the loss of hydrophobic contacts in the binding locations of DA and AA-DA which is more intense in the AA-DA binding, as this ligand binds to the hydrophobic calyx and spoils the hydrophobic interactions between the close contact residues of the calyx. This is in good agreement with the R<sub>g</sub> results which showed the less compactness of BLG in BLG-(AA-DA) complex in comparison with the BLG in BLG-(DA) complex.

**Hydrogen bond.** Hydrogen bond is one of the main forces in ligand binding process which its strength in biological systems varies between 5-30 kJ mol<sup>-1</sup>, and subsequently, they can be formed and broken quickly during binding process, conformational changes, or protein folding. Accordingly, hydrogen bonds in biological conditions may be broken/formed with energies that are within the range of thermal fluctuations. This is one of the main factors facilitating macromolecular association events, and biological activity. The number and stability of H-bonds between protein and ligand is an important factor contributing to the stability of ligand binding.

The presence of H-bonds between ligands and protein was calculated every 5 ps using the g\_hbond module of GROMACS. The results of simulation revealed that two H-bonds between DA and Glu44 and His161 of BLG maintain in the whole time of simulation whereas the H-bonds between DA and Gln59 maintain in 68% of the simulation time. Also, some other H-bonds between DA and Trp19, Ser20, Glu157, and Glu158 were formed, due to the slight rotation of ligand respect to the protein. The only H-bond between AA-DA and BLG vanished at the initial steps of the analyzing trajectory, while the strong H-bonds between Asn88, Glu89, and Ser110 and ligand were formed at approximately 5000 ps and conserved in the rest of the simulation time, which implied the rotation of AA-DA in

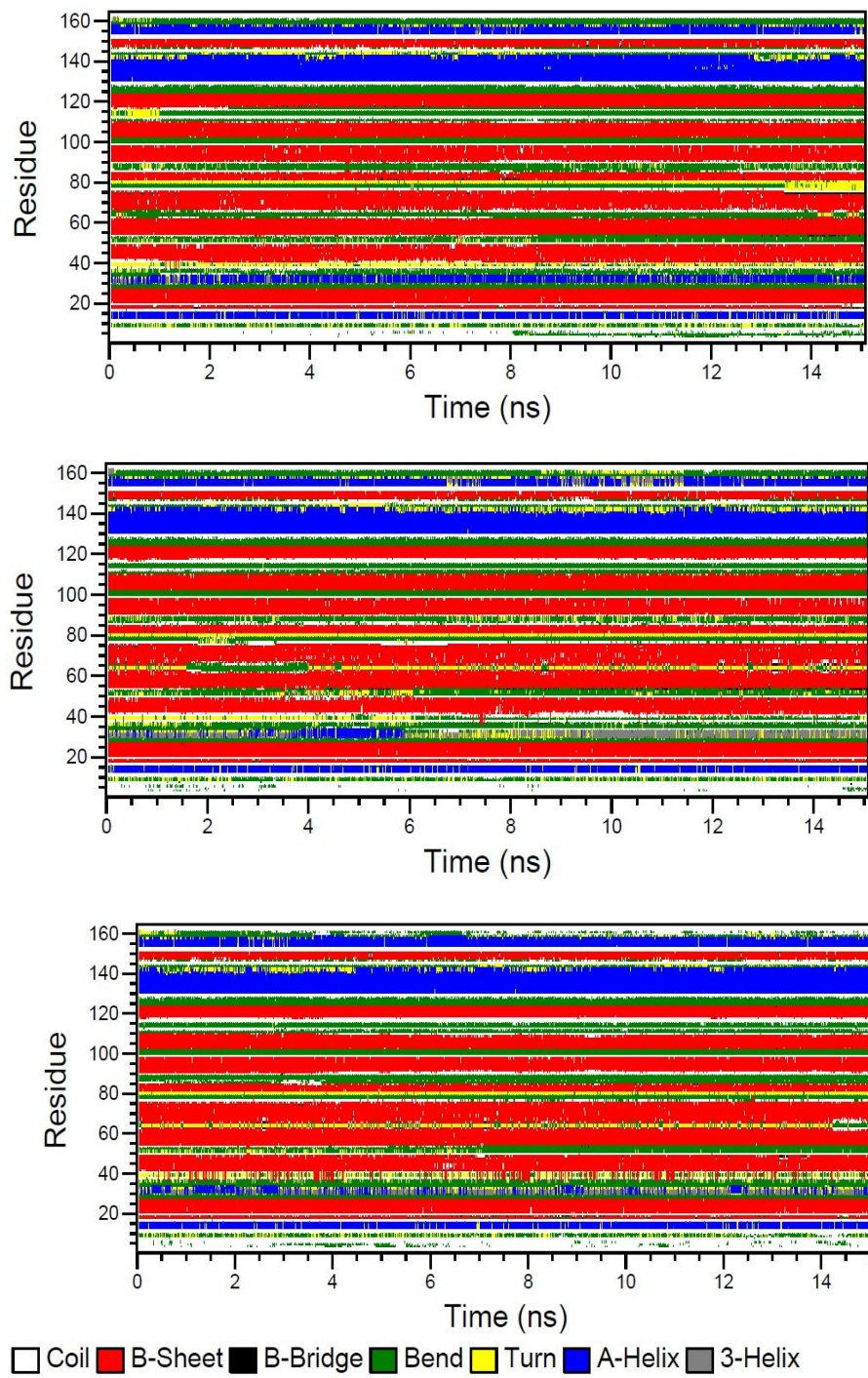
the binding site and the importance of H-bond interactions in the binding process.

**Secondary structure.** Additional information on the structural flexibility of protein during the binding process is obtained by the analysis of time-dependent secondary structure fluctuations. The evaluation of changes in the secondary structure during the simulation time can lead us to obtain precious information regarding protein stability. The secondary structure of BLG before and after the binding was calculated with the DSSP code [37]. The program generated Fig. 7 that represents the secondary structure contents of free and bound BLG with DA and AA-DA during the simulation. The results indicate that the more important secondary structure contents, beta-sheets and alpha-helices, were conserved throughout the simulation period for both free and bound protein which signifies not only the stability of free protein trajectory during the simulation time, but also, the insignificant change of secondary structure due to the binding of DA and AA-DA.

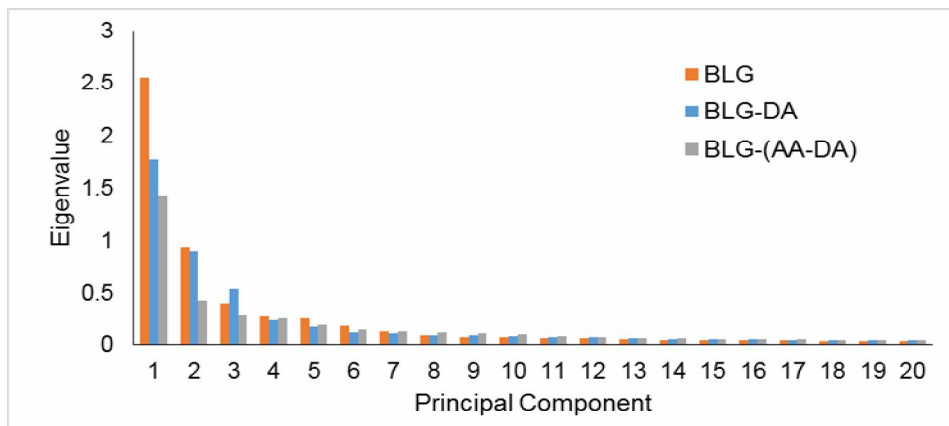
**Principal component analysis (PCA).** PCA transforms the original space of correlated variables into a reduced space of independent variables (*i.e.* principal components or eigenvectors). In a system of  $N$  atoms, there are  $3N-6$  modes of possible internal fluctuations (six degrees of freedom are required to describe the external rotation and translation of the system). PCA or essential dynamics simulation, in other word, divides the conformational space of the protein into two subspaces, an essential subspace and a nonessential, physically constrained subspace [38]. In the essential subspace, positional fluctuation of the atoms is defined by the unconstrained, anharmonic motion, therefore, it helps us to determine what motions contribute most to the overall dynamics of the protein. In Gromacs, the covariance matrix,  $C$ , of the atomic coordinates is used to obtain the PCs:

$$C_{ij} = \langle M_i^{1/2}(x_i - \langle x_i \rangle) M_j^{1/2}(x_j - \langle x_j \rangle) \rangle$$

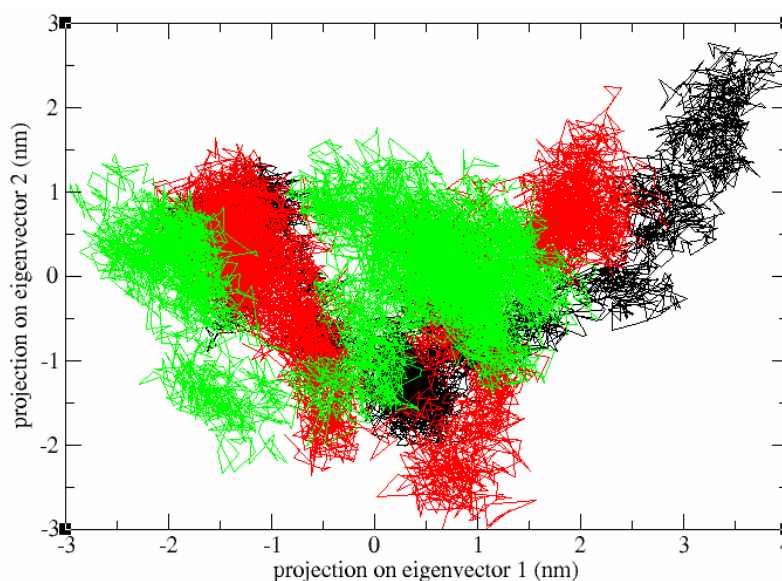
where,  $M$  is a diagonal matrix containing the masses of the atoms (mass-weighted analysis) or the unit matrix (non-mass weighted analysis). The amplitude and direction of dominant protein motions are identified by the calculation of eigenvectors and eigenvalues of covariance matrix. To further characterize the behavior of protein and complexes in the essential subspace, the PCA based on the MD



**Fig. 7.** Variation of the secondary structure of protein vs. time for free (top) and bound BLG with DA (middle) and AA-DA (bottom), during the 15 ns simulation. The plots were prepared using DSSP program.



**Fig. 8.** The obtained eigenvalue quantity distribution from MD trajectory, for the first 20 eigenvectors of free and bound protein with DA and AA-DA ligands.



**Fig. 9.** 2-D projection of the first two principal components for BLG (black), BLG-DA (red) and BLG-(AA-DA) (green). The dissimilar distribution patterns confirm the existence of different principal motions and therefore, non-identical binding sites for DA and AA-DA.

trajectories have been performed and the results are displayed in Fig. 8. The x-axis represents the first 20 principal eigenvectors, while the y-axis shows the eigenvalue of the corresponding eigenvector (principal component). With respect to this figure, the first few

eigenvectors (modes of fluctuation) with the largest associated eigenvalues are more informative and define the essential subspace in which most of the protein dynamics occurs, while the latter components carry little information about the protein and complex motion (Fig. 8). Also, the

results revealed that first ten PCs can explain 75.97%, 69.80% and 64.02% of the observed variance in the MD simulation, and therefore the global motions, in the case of BLG, BLG-DA, and BLG-(AA-DA), respectively. Figure 9 represents the bi-dimensional projections of the first two PCs for free and bound protein and verifies that BLG covers a larger region of phase space, particularly along PC1 plane, compared to that covered by complexes. Global flexibility of the protein in both free and bound states was further inspected by the trace of the diagonalized covariance matrix of the  $C\alpha$  atomic positional fluctuations. This quantity for the free protein was  $6.57 \text{ nm}^2$  while for complexes BLG-DA and BLG-(AA-DA), a smaller values,  $5.91 \text{ nm}^2$  and  $5.00 \text{ nm}^2$  was observed, respectively, and thus, confirming the overall decreased flexibility of bound proteins compared to the free protein which is consistent with RMSD plots. 2-D projection of PC1 vs. PC2 patterns are completely different for both compounds; representing the variance of their principal motions in the binding process which implies the existence of dissimilar binding site for DA and AA-DA and verifying the docking results.

## CONCLUSIONS

Binding of DA and AA-DA with BLG, have been studied using molecular docking and molecular dynamics simulation. Molecular docking calculations indicated that in contrast to dopamine which binds to the outer surface site, AA-DA binds to the hydrophobic pocket, calyx, on the basis of hydrophobic interactions of its lipophilic long chain with the calyx residues, namely, Val, Leu, Ile, Phe, Asn, Met, Glu and, Gln. Despite the importance of hydrogen bond and charge interactions in the DA binding case, more accurate docking with  $60 \times 60 \times 60$  docking box manifested the major participation of hydrophobic forces to the binding interaction of AA-DA to BLG.

The RMSD convergence of trajectory together with the  $R_g$  profile from MD simulations established the stability of BLG-ligand complexes and validity of docking results. Secondary structures together with the gyration radius data represented insignificant changes in the structure of BLG due to the binding of DA and AA-DA. The RMSF profiles of free and bound BLG residues and H-bond analysis revealed slight movement of ligands from their docking

pose during the MD simulation. SASA calculations disclosed the impact of the binding on the protein structure in terms of increasing the solvent exposure due to the loss of hydrophobic contacts in the binding locations of DA and AA-DA which is more intense in the AA-DA binding. Computational results represent the binding of catecholamines with negligible changes in structure and dynamics of the protein and therefore, potency of BLG as suitable carrier for transporting of these pharmaceutically important compounds *in vitro*. As AA-DA binds to the hydrophobic calyx of BLG rather than the outer surface, which is the case in the DA binding site, this protein transporter could be considered as more protective carrier of AA-DA with respect to DA.

## ACKNOWLEDGMENTS

The financial support of the Research Council of University of Isfahan and Iran National Science Foundation (grand number 93013717) are gratefully acknowledgment.

## Author Contributions

The contribution of authors are as follows:

- 1) S. Gholami: performed research; contributed analytic tools; analyzed data
- 2) A. K. Bordbar: performed research; wrote the paper

## REFERENCES

- [1] Akimov, M.; Bezuglov, V., N-Acylated Dopamines: A New Life for the Old Dopamine. Dopamine: Functions, Regulation and Health Effects. New York: 2012, p. 49-80.
- [2] Goldberg, L. I., Cardiovascular and renal actions of dopamine: potential clinical applications. *Pharmacol. Rev.* **1972**, *24*, 1-29.
- [3] Moncrief, J., The Myth of the Chemical Cure: A Critique of Psychiatric Drug Treatment. Macmillan: 2008, p. 21.
- [4] Akimov, M.; Ashba, A.; Gretskeya, N.; Bezuglov, V. In some aspects of the mechanism of cell death induction by the lipids of N-Acyl Dopamine family in the PC12 cancer cell line. *Anticancer Research*: 2014; p. 5797-5800.



- [5] Dhalla, N. S.; Adameova, A.; Kaur, M., Role of catecholamine oxidation in sudden cardiac death. *Fundam. Clin. Pharmacol.* **2010**, *24*, 539-546, DOI: 10.1111/j.1472-8206.2010.
- [6] Bittner, S., When quinones meet amino acids: chemical, physical and biological consequences. *Amino Acids* **2006**, *30*, 205-224, DOI: 10.1007/s00726-005-0298-2.
- [7] Halpin, M. I.; Richardson, T., Selected functionality changes of  $\beta$ -Lactoglobulin upon esterification of side-chain carboxyl groups. *J. Dairy Sci.* **1985**, *68*, 3189-3198, DOI: 10.3168/jds.S0022-0302(85)81226-1.
- [8] Liang, L.; Subirade, M.,  $\beta$ -Lactoglobulin/folic acid complexes: formation, characterization, and biological implication. *J. Phys. Chem. B* **2010**, *114*, 6707-6712, DOI: 10.1021/jp101096r.
- [9] Liang, L.; Tajmir-Riahi, H.; Subirade, M., Interaction of  $\beta$ -lactoglobulin with resveratrol and its biological implications. *Biomacromolecules* **2007**, *9*, 50-56, DOI: 10.1021/bm700728k.
- [10] Mensi, A.; Choiset, Y.; Rabesona, H.; Haertlé, T.; Borel, P.; Chobert, J. -M., Interactions of  $\beta$ -lactoglobulin variants A and B with vitamin A. Competitive binding of retinoids and carotenoids. *J. Agric. Food Chem.* **2013**, *61*, 4114-4119, DOI: 10.1021/jf400711d.
- [11] Stanić-Vučinić, D.; Ćirković-Veličković, T., The modifications of bovine  $\beta$ -lactoglobulin: Effects on its structural and functional properties. *J. Serb. Chem. Soc* **2013**, *78*, 445-461, DOI: 10.2298/JSC120810155S.
- [12] Shpigelman, A.; Israeli, G.; Livney, Y. D., Thermally-induced protein-polyphenol co-assemblies: beta lactoglobulin-based nanocomplexes as protective nanovehicles for EGCG. *Food Hydrocoll* **2010**, *24*, 735-743, DOI: 10.1016/j.foodhyd.2010.03.015.
- [13] Taheri+Kafrani, A.; Choiset, Y.; Faizullin, D. A.; Zuev, Y. F.; Bezuglov, V. V.; Chobert, J. M.; Bordbar, A. K.; Haertlé, T., Interactions of  $\beta$ -lactoglobulin with serotonin and arachidonyl serotonin. *Biopolymers* **2011**, *95*, 871-880, DOI: 10.1002/bip.21690.
- [14] Gholami, S.; Bordbar, A.; Akvan, N.; Parastar, H.; Fani, N.; Gretskeya, N.; Bezuglov, V.; Haertlé, T., Binding assessment of two arachidonic-based synthetic derivatives of adrenalin with  $\beta$ -lactoglobulin: Molecular modeling and chemometrics approach. *Biophys. Chem.* **2015**, *207*, 97-106, DOI: 10.1016/j.bpc.2015.10.001.
- [15] Frisch, M.; Trucks, G.; Schlegel, H.; Scuseria, G.; Robb, M.; Cheeseman, J.; Montgomery Jr, J.; Vreven, T.; Kudin, K.; Burant, J.; Gaussian 03, R. B., Gaussian, Inc., Wallingford, CT, **2004**. Gaussian 03, Revision B. 05, MJ Frisch, *et al.* Gaussian. Inc., Pittsburgh, PA . 2003.
- [16] Morris, G. M.; Goodsell, D. S.; Halliday, R. S.; Huey, R.; Hart, W. E.; Belew, R. K.; Olson, A. J., Automated docking using a Lamarckian genetic algorithm and an empirical binding free energy function. *J. Comput. Chem.* **1998**, *19*, 1639-1662, DOI: 10.1002/(SICI)1096-987X(19981115)19:14<1639::AID-JCC10>3.0.CO;2-B.
- [17] Berendsen, H. J.; Postma, J.; Van Gunsteren, W.; Hermans, J., Interaction Models for Water in Relation to Protein Hydration. Springer: 1981, p. 331-342.
- [18] Van Der Spoel, D.; Lindahl, E.; Hess, B.; Groenhof, G.; Mark, A. E.; Berendsen, H. J., GROMACS: fast, flexible, and free. *J. Comput. Chem.* **2005**, *26*, 1701-1718, DOI: 10.1002/jcc.20291.
- [19] Van Gunsteren, W. F.; Billeter, S.; Eising, A.; Hünenberger, P. H.; Krüger, P.; Mark, A. E.; Scott, W.; Tironi, I. G., Biomolecular Simulation: The {GROMOS96} Manual and User Guide. 1996,
- [20] Schuttelkopf, A. W.; Van Aalten, D. M., PRODRG: a tool for high-throughput crystallography of protein-ligand complexes. *Acta Crystallogr., Sect. B: Struct. Sci.* **2004**, *60*, 1355-1363, DOI: 10.1107/S0907444904011679.
- [21] Darden, T.; York, D.; Pedersen, L., Particle mesh Ewald: An  $N \log(N)$  method for Ewald sums in large systems. *J. Chem. Phys.* **1993**, *98*, 10089-10092, DOI: 10.1063/1.464397.
- [22] Essmann, U.; Perera, L.; Berkowitz, M. L.; Darden, T.; Lee, H.; Pedersen, L. G., A smooth particle mesh Ewald method. *J. Chem. Phys.* **1995**, *103*, 8577-8593, DOI: 10.1063/1.470117.
- [23] Nosé, S., A molecular dynamics method for



- simulations in the canonical ensemble. *Mol. phys* **1984**, *52*, 255-268, DOI: 10.1080/00268978400101201.
- [24] Hoover, W. G., Canonical dynamics: equilibrium phase-space distributions. *Phys. Rev. A* **1985**, *31*, 1695, DOI: 10.1103/PhysRevA.31.1695.
- [25] Parrinello, M.; Rahman, A., Polymorphic transitions in single crystals: A new molecular dynamics method. *J. Appl. phys.* **1981**, *52*, 7182-7190, DOI: 10.1063/1.328693.
- [26] Hockney, R. W., Potential calculation and some applications; Langley Research Center, Hampton, Va.: 1970.
- [27] Muresan, S.; van der Bent, A.; de Wolf, F. A., Interaction of  $\beta$ -lactoglobulin with small hydrophobic ligands as monitored by fluorometry and equilibrium dialysis: nonlinear quenching effects related to protein-protein association. *J. Agric. Food. Chem.* **2001**, *49*, 2609-2618, DOI: 10.1021/jf0012188.
- [28] Wu, S. -Y.; Pérez, M. D.; Puyol, P.; Sawyer, L.,  $\beta$ -Lactoglobulin binds palmitate within its central cavity. *J. Biol. Chem.* **1999**, *274*, 170-174, DOI: 10.1074/jbc.274.1.170.
- [29] Ragona, L.; Pusterla, F.; Zetta, L.; Monaco, H. L.; Molinari, H., Identification of a conserved hydrophobic cluster in partially folded bovine  $\beta$ -lactoglobulin at pH 2. *Fold. Des.* **1997**, *2*, 281-290, DOI: 10.1016/S1359-0278(97)00039-4.
- [30] Roufik, S.; Gauthier, S. F.; Leng, X.; Turgeon, S. L., Thermodynamics of binding interactions between bovine  $\beta$ -lactoglobulin A and the antihypertensive peptide  $\beta$ -Lg f142-148. *Biomacromolecules* **2006**, *7*, 419-426, DOI: 10.1021/bm050229c.
- [31] Yang, M. C.; Guan, H. H.; Liu, M. Y.; Lin, Y. H.; Yang, J. M.; Chen, W. L.; Chen, C. J.; Mao, S. J., Crystal structure of a secondary vitamin D3 binding site of milk  $\beta$ -lactoglobulin. *Proteins: Struct Func Bioinformat* **2008**, *71*, 1197-1210, DOI: 10.1002/prot.21811.
- [32] Evoli, S.; Guzzi, R.; Rizzuti, B., Molecular simulations of  $\beta$ -lactoglobulin complexed with fatty acids reveal the structural basis of ligand affinity to internal and possible external binding sites. *Proteins: Struct. Func. Bioinformat.* **2014**, *82*, 2609-2619, DOI: 10.1002/prot.24625.
- [33] Pantusa, M.; Bartucci, R.; Rizzuti, B., Stability of trans-resveratrol associated with transport proteins. *J. Agric. Food. Chem.* **2014**, *62*, 4384-4391, DOI: 10.1021/jf405584a.
- [34] Wu, X.; Dey, R.; Wu, H.; Liu, Z.; He, Q.; Zeng, X., Studies on the interaction of epigallocatechin+3+gallate from green tea with bovine  $\beta$ -lactoglobulin by spectroscopic methods and docking. *Int. J. Dairy. Tech* **2013**, *66*, 7-13, DOI: 10.1111/j.1471-0307.2012.00873.x
- [35] Sawyer, L.; Kontopidis, G., The core lipocalin, bovine  $\beta$ -lactoglobulin. *BBA-Protein Struct. M* **2000**, *1482*, 136-148, DOI: 10.1016/S0167-4838(00)00160-6.
- [36] Lee, B.; Richards, F. M., The interpretation of protein structures: estimation of static accessibility. *J. Mol. Biol.* **1971**, *55*, 379-IN4, DOI: 10.1016/0022-2836(71)90324-X.
- [37] Kabsch, W.; Sander, C., Dictionary of protein secondary structure: pattern recognition of hydrogen-bonded and geometrical features. *Biopolymers* **1983**, *22*, 2577-2637, DOI: 10.1002/bip.360221211.
- [38] Amadei, A.; Linssen, A.; Berendsen, H. J., Essential dynamics of proteins. *Proteins: Struct. Func. Bioinformat.* **1993**, *17*, 412-425, DOI: 10.1002/prot.340170408.